

Elucidation of Diels–Alder Reaction Network of 2,5-Dimethylfuran and Ethylene on HY Zeolite Catalyst

Phuong T. M. Do,^{†,§,⊥} Jesse R. McAtee,^{‡,⊥} Donald A. Watson,^{*,‡} and Raul F. Lobo^{*,†}

Catalysis Center for Energy Innovation,[†] Department of Chemical & Biomolecular Engineering, and [‡]Department of Chemistry and Biochemistry University of Delaware, Newark, Delaware 19716, United States

Supporting Information

ABSTRACT: The reaction of 2,5-dimethylfuran and ethylene to produce *p*-xylene represents a potentially important route for the conversion of biomass to high-value organic chemicals. Current preparation methods suffer from low selectivity and produce a number of byproducts. Using modern separation and analytical techniques, the structures of many of the byproducts produced in this reaction when HY zeolite is employed as a catalyst have been identified. From these data, a detailed reaction network is proposed, demonstrating that hydrolysis and electrophilic alkylation reactions compete with the desired Diels–Alder/dehydration sequence. This information will allow the rational identification of more selective catalysts and more selective reaction conditions.

KEYWORDS: *p*-xylene, biomass, 2,5-dimethylfuran, ethylene, 2D-NMR, reaction network, zeolite

1. INTRODUCTION

The high cost, market volatility, and limited availability of petroleum-based feedstocks for fuel and chemical production, in addition to the pressing need to find energy sources that minimize societal impact on climate change, have motivated much research into developing second-generation biomass or nonfood lignocellulosic feedstocks as substitutes for fossil fuels.^{1,2} Processing of biomass, however, has many challenges, including the effective conversion of biomass-derived oxygenates into valuable products, the identification of novel catalytic routes to produce useful chemicals, and the design of effective catalysts for these chemistries.³ Another challenge is that the reaction database and analytical capabilities that have been established for traditional hydrocarbon processing are not effective for dealing with oxygen-containing compounds such as biomass oxygenates. The analytical methods needed to determine the reaction intermediates, products, and byproducts rank then as one of the highest priorities in biomass process engineering and design. In other words, the conceptual design of a biomass process cannot be achieved without knowing many details of the reaction network that takes reagents to products.

Recently,⁴ one of our groups has reported a “green” route to catalytically convert 2,5-dimethylfuran (DMF) and ethylene to *p*-xylene, an important precursor for the manufacture of polyethylene terephthalate.⁵ Both ethylene and DMF can be derived from lignocellulose feedstocks.^{6,7} An important characteristic feature of this catalytic route is that *p*-xylene is the sole xylene isomer that is synthesized, reducing the high costs of mixed xylene purification required by the existing production infrastructure.⁸ The pathway from DMF to *p*-

xylene, depicted in Figure 1, proceeds through a two-step reaction: Diels–Alder cycloaddition of DMF and ethylene,

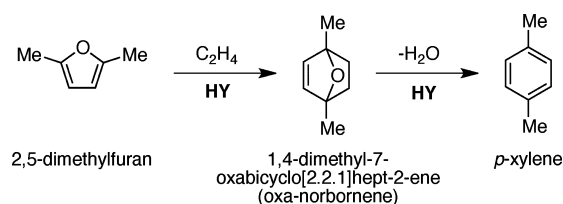


Figure 1. Synthesis of *p*-xylene from 2,5-dimethylfuran and ethylene on HY zeolite (Si/Al = 2.55).

followed by the dehydration of the oxa-norbornene intermediate. The use of Brønsted acid zeolites provides much higher yields of *p*-xylene compared with results reported in the literature.^{9,10} On HY zeolite at 573 K, ~60% selectivity for *p*-xylene is observed at 95% conversion of DMF. Further enhancement of the selectivity (75% based on DMF) was observed using *n*-heptane as solvent; however, similarly to other reactions related to the processing of biomass-derived compounds,^{11–13} a fraction of uncharacterized byproducts was formed. These unknown byproducts result in a reduction of the selectivity to *p*-xylene.⁴

Establishing an experimental protocol that, in combination with state-of-the-art analytical tools, can identify the chemical structure of the unknown byproducts and thereby elucidate the

Received: October 15, 2012

Revised: December 3, 2012

Published: December 12, 2012

reaction pathways leading to these side products is crucial. This new information will also clarify how best to select the reaction operating variables and rationally choose catalysts to maximize the production of *p*-xylene. In addition, a report by the DOE Office of Basic Science identified the understanding of mechanisms and dynamics of catalyzed transformations as the first grand challenge in general catalysis, particularly for biomass conversion.¹⁴

In fact, ¹H and ¹³C nuclear magnetic resonance (NMR) spectroscopy and gas chromatography/mass spectrometry (GC/MS) are common analytical techniques in organic synthesis, natural products isolation, and other fields.^{15–19} However, for mixtures of closely related isomers or polymer structures, overlapping of ¹H NMR or ¹³C NMR signals often occurs, complicating the identification of important side products of the reaction mixture. The combination of organic separation techniques and two-dimensional NMR (based on homonuclear and heteronuclear correlations) are effective in resolving the issues associated with overlapping signals; however, these sophisticated analytical techniques have been applied only to a limited extent in the identification of uncharacterized products and intermediates and generally to the overall reaction network of biomass derived compounds.²⁰ For example, the tools used to identify the compounds produced during fast pyrolysis of carbohydrate and cellulose feedstocks have been characterized solely by electron ionization in GC/MS and retention-time validation with commercial standards.^{12,21}

Here, for the first time, we report the determination of a (nearly) complete reaction network for the cycloaddition reaction of 2,5-dimethylfuran and ethylene on the heterogeneous catalyst HY zeolite using a combination of classical separation techniques, high-resolution GC/MS, and multi-dimensional NMR spectroscopy. The objective has not been to maximize the yield of *p*-xylene, but rather, to capitalize on the formation of dominant side products using mild reaction conditions. The dominant side products were found to result from the electrophilic reactions of cationic intermediates with DMF and other nucleophiles in the reaction. The observed chemistry on acidic HY zeolite includes Diels–Alder, dehydration, Friedel–Crafts-type alkylation, and hydrolysis via Brønsted acid sites. Finally, solutions to operating modes and zeolitic catalyst design principles to minimize side product formation have been proposed.

2. EXPERIMENTAL SECTION

2.1. Catalytic Reactions. It is essential to purify DMF (99% from Sigma-Aldrich) by distillation to eliminate heavy contaminants. The distillate is stored in an oxygen- and water-free glovebox prior to reaction measurements. Zeolite HY (25 mg, Si/Al = 2.55 from Zeolyst International, CBV 600) and DMF (8 mL) were charged into a 45 mL closed Parr reactor (series 4703-4714, General Purpose Pressure Vessels) under Ar atmosphere inside a dry and oxygen-free glovebox. The container was then filled with ethylene to a total pressure of 4.69 MPa (Scotts Specialty Gas, Inc., 99.5% purity) and heated using a Chemglass oil-bath unit to 493 or 528 K for 6 h. Mixing inside the reactor was accomplished by using a magnetic stirrer. A reaction using a mixture of 3 mL of deuterated *d*₁₀-*p*-xylene and 8 mL of DMF and a reaction using 8 mL of pure 2,5-hexanedione were also carried out using the same protocol. At the end of the reaction period, the reactor was cooled in an ice bath for 30 min, and the products were collected, filtered

through a 0.2 μm syringe filter, and diluted with methylene chloride for analysis using a Shimadzu GC 2010 Plus equipped with a Thermo Scientific TR-1 column (10 m × 0.1 mm, i.d. 0.1 μm film).²²

To isolate the polar compounds from the crude reaction mixture, the volatile components (including DMF and xylene) were removed on a rotary evaporator. The residue was then subjected to preparative flash chromatography on silica gel. Isolated products were then analyzed by a combination of techniques to determine their chemical structure.

2.2. Analytical. 400 MHz ¹H and 100 MHz ¹³C NMR spectra were measured on a 400 MHz FT-NMR spectrometer equipped with a Bruker S2 CryoPlatform in the indicated deuterio solvent and at ambient temperature. Chemical shifts are reported in parts per million. Residual CHCl₃ (from CDCl₃) was used as a reference for chemical shifts. ¹H/¹³C HMBC (heteronuclear multiple bond correlation), ¹H/¹³C HMQC (heteronuclear multiple quantum correlation) and ¹H COSY (homonuclear correlation spectroscopy) NMR experiments were recorded, as well.

Two-dimensional NMR cross-signals were assigned by combining the results of the different experiments. Structural elucidation of some compounds was obtained from 1D- and 2D-NMR spectral data in combination with GC/MS data collected using an Agilent 6850 series GC and 5973 MS detector. High-resolution (HR) MS was obtained at the University of California (UC), Irvine, using their Micromass Autospec with EI+ used to provide exact chemical formulas.

The separation of most compounds was achieved using flash silica gel chromatography eluting with hexanes, followed by a gradient to 50% ethyl ether in hexanes. Analytical thin-layer chromatography (TLC) was performed on precoated glass plates and visualized by UV or by staining with KMnO₄ or ceric ammonium molybdate. Further flash silica gel chromatographic purification was necessary for many of the minor isolates, as described in the Supporting Information.

3. RESULTS AND DISCUSSION

3.1. Product Identification. Figure 2 shows a typical gas chromatogram of the reaction mixture after the reaction of

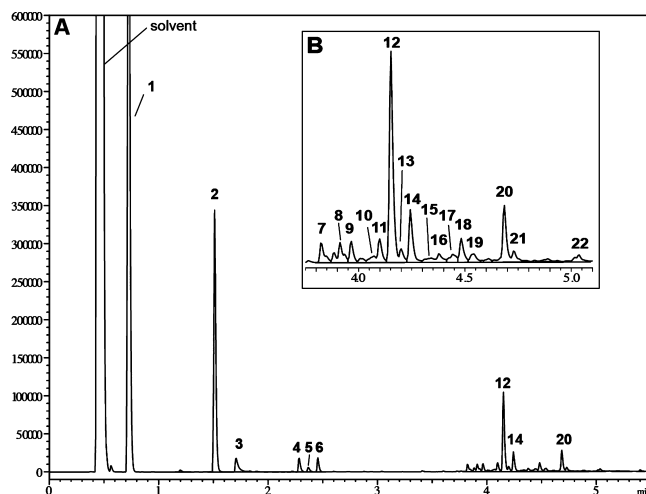
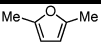
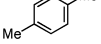
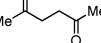
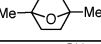
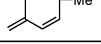
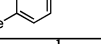
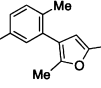
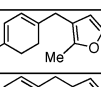
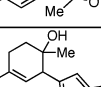
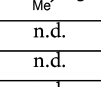
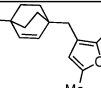
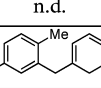
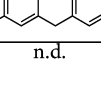


Figure 2. (A) Gas chromatogram of all liquid products from reaction of 2,5-dimethylfuran and ethylene over HY (Si/Al = 2.55) at 528 K. (B) Expanded region showing heavy products. Peak numbers correspond to compounds listed in Table 1.

DMF with ethylene on HY zeolite over a range of temperatures (493–528 K). A total of 22 compounds (including DMF) were identified in the mixture using this analytical technique. The GC area percentile, chemical structure, and chemical formulas are summarized in Table 1.

Table 1. Product Distribution of Reaction of 2,5-Dimethylfuran and Ethylene over HY Zeolite^a

compound	area % 493 K	area % 528 K	chemical formula	chemical structure
1	88.9	70.3	C ₆ H ₈ O	
2	5.3	15.9	C ₈ H ₁₀	
3	0.3	1.4	C ₆ H ₁₀ O ₂	
4	0.0	0.9	C ₈ H ₁₂ O	
5	0.4	0.3	C ₈ H ₁₂ O	
6	0.3	0.8	C ₁₀ H ₁₄	
7	0.2	0.4	C ₁₄ H ₁₈ O	n.d.
8	0.1	0.3	C ₁₄ H ₁₈ O	n.d.
9	0.1	0.4	C ₁₄ H ₂₀ O ₂	n.d.
10	0.2	0.2	C ₁₄ H ₁₆ O	
11	0.3	0.5	C ₁₄ H ₂₀ O ₂	n.d.
12	1.9	4.2	C ₁₄ H ₁₈ O	
13	0.2	0.1	C ₁₄ H ₁₆ O	
14	0.7	1.0	C ₁₄ H ₂₀ O ₂	
15	0.1	0.2	C ₁₆ H ₁₈	n.d.
16	0.2	0.2	C ₁₄ H ₂₀ O ₂	n.d.
17	0.2	0.3	n.d.	n.d.
18	0.2	0.5	C ₁₆ H ₂₂ O	
19	0.2	0.3	C ₁₄ H ₁₆ O ₂	n.d.
20	0.1	1.2	C ₁₆ H ₂₀	
21	0.1	0.4	C ₁₆ H ₁₈	
22	0.1	0.2	C ₁₄ H ₁₆ O ₂	n.d.

^an.d. = not determined; % area determined using GC-FID and are uncorrected. Where structure is unknown, molecular formulas are proposed on the basis of GC/MS analysis of the crude reaction mixture.

A number of compounds, particularly those that were volatile, were identified by coinjection of commercial standards using both GC/FID and GC/MS. These include DMF (1), *p*-xylene (2), 2,5-hexanedione (3), and 1-methyl-4-propylbenzene (6). The retention times and mass patterns of these compounds matched the known standards; the details of these

analyses can be found in the Supporting Information (Figures SI-5, SI-6, SI-7, and SI-8). The presence of these compounds in the crude reaction mixture was also confirmed using ¹H NMR.

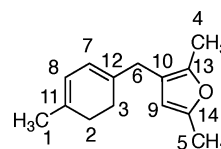
For compounds 4 and 5, the use of coinjection standards to confirm identity was not possible; however, GC/MS (Supporting Information Figure SI-8) revealed a parent ion of 124 *m/z*, with similar fragmentation patterns for both compounds. This molecular ion corresponds to a molecular formula of C₈H₁₂O, which is consistent with the intermediate oxanorbornene or isomers thereof. On the basis of the retention time, we tentatively assign compound 4 as the oxanorbornene, as shown in Table 1. On the basis of analysis of the other reaction products (described below), we have assigned compound 5 as the isomeric alcohol resulting from protolytic ring-opening of the bridging ether and loss of proton from the sterically accessible methyl group. This compound is a possible intermediate en route to *p*-xylene. Consistent with this assignment, attempts to isolate compound 5 were unsuccessful and resulted in only the isolation of *p*-xylene (as determined by ¹H NMR), which strongly suggests that it is, in fact, an intermediate en route to the final product.

For less volatile components, we were successful in isolating several compounds using flash column chromatography. These included compounds 10, 12, 14, 18, and 20, which were of sufficient purity for subsequent structural assignment. Comparison of the GC/MS and ¹H NMR spectra of the isolated materials with those of the crude reaction mixtures confirmed that the isolated compounds were significant components of the crude mixture. Single- and multidimensional NMR spectra of these species were collected (including ¹H, ¹³C, COSY, NOESY, HMQC, HMBC).

These spectra can be found in the Supporting Information. The NMR correlations for compound 12 are summarized in Table 2 and are representative of the data collected in this study. From this analysis, we have assigned compound 12 as the bicyclic diene shown. Using similar techniques, the

Table 2. Summary of 1D and 2D NMR Data of Compound 12

carbon number	type	¹ H NMR (ppm)	¹³ C NMR (ppm)	COSY	HMBC
1	CH ₃	1.75	23	6, 7, 8	3, 7, 8, 11
2	CH ₂	2.08	27	6	3, 7, 8, 11, 12
3	CH ₂	2.08	29	6	2, 7, 8, 11, 12
4	CH ₂	2.17	12		10, 13
5	CH ₂	2.21	14	9	9, 14
6	CH ₂	3.00	33	1, 2, 3, 7, 8	2, 7, 8, 9, 12, 13
7	CH	5.58	119	1, 2, 3, 6	2, 3, 6, 8, 11, 12
8	CH	5.58	119	1, 2, 3, 6	1
9	CH	5.74	108	5	10, 13, 14
10	C		117		
11	C		133		
12	C		135		
13	C		146		
14	C		149		



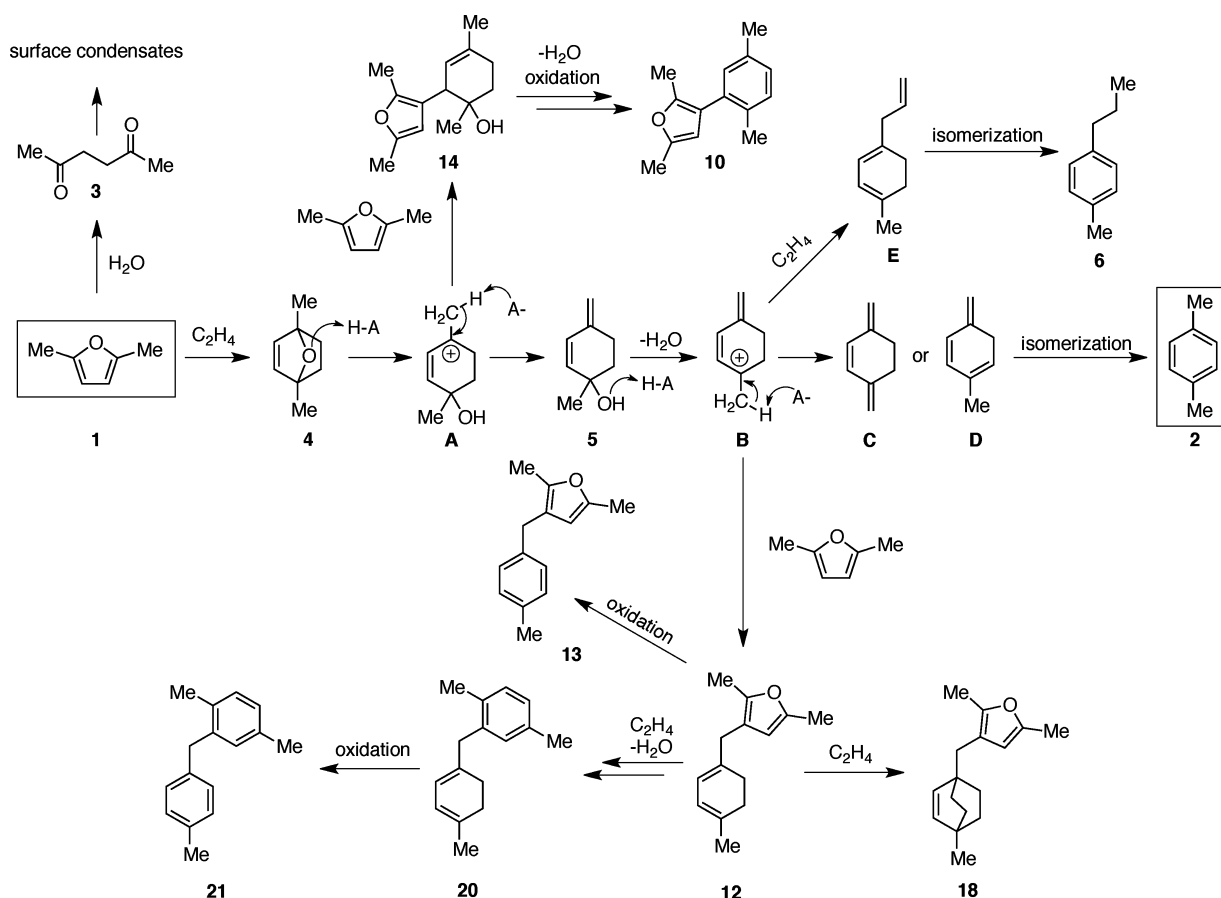


Figure 3. Detailed reaction network of 2,5-dimethylfuran and ethylene at 4.69 MPa of ethylene and 528 K.

structures of compounds **10**, **14**, **18**, and **20** were assigned. The structures of these compounds are given in Table 1.

Finally, we observed that as samples of the crude mixture were allowed to age under air, compounds **13** and **21** appeared to increase in abundance at the expense of compounds **12** and **20**. We were able to isolate samples of **13** and **21** and assign their structures as the aromatic compounds shown in Table 1. In addition, we note that isolated samples of **12** and **20** were also converted to **13** and **21** upon standing in air.

For the other components of the crude reaction mixture, we were unable to isolate samples of sufficient quantity and purity to allow structural assignment; however, the majority of the remaining compounds are relatively minor components of the crude reaction mixture. Further, although we were unable to fully assign the structures of these products, GC/MS analysis of the reaction mixtures revealed mass spectral fragmentation patterns of the unassigned materials similar to those compounds shown in Table 1, suggesting that these minor components are closely related isomers and likely produced via similar mechanistic pathways.

In total, we were able to identify 13 of 22 compounds in the crude reaction mixture, including 10 of 11 of the most abundant components from the reactions performed at 528 K.

3.2. Analysis of Reaction Network of 2,5-Dimethylfuran and Ethylene over HY Zeolite. The structures of the assigned compounds allow understanding of the reaction network of this transformation (Figure 3). As shown in a previous report, the Diels–Alder reaction of DMF and ethylene is enhanced by the confinement effect inside the zeolite pores.²³

The Diels–Alder reaction leads to oxanorbornene intermediate **4**.

Dehydration of intermediate **4** requires an acid catalyst; in this case, the HY zeolite. Protonation of the ether of **4** and subsequent ring-opening leads to allylic cation **A**. Deprotonation of **A** at the exocyclic methyl group is expected because it is the least sterically encumbered position adjacent to the cation. This pathway leads to formation of alcohol **5**. Alternatively, cation **A** can participate in a Friedel–Crafts-type reaction with DMF, leading to compound **14**. The regiochemistry in this reaction is explained as the addition to the less-substituted site of the allyl cation.

The intermediacy of compound **5** is further supported by the structures of downstream products. Protonation of the alcohol of **5**, followed by dehydration, leads to the highly stabilized pentadienyl cation **B**. Deprotonation of this cation leads to the desired *p*-xylene (**2**). Our hypothesis is that the site of kinetic deprotonation is the exocyclic methyl group, leading to the extended triene **C**; however, we cannot rule out the formation of **D** as the intermediate. In either case, both **C** and **D** would be expected to quickly isomerize to *p*-xylene under the acidic conditions, driven by the exothermicity of aromatization.

This desired pathway to **2** also generates an equivalent of water, likely responsible for the observed formation of 2,5-hexanedione (**3**). It is well-known that DMF can be hydrated in acidic media to give this diketone.²⁴ Further, dione **3** is also prone to acid-catalyzed aldol polymerization, which may explain the observed polymeric surface condensates.

Cation **B** can also react through a number of undesired electrophilic pathways. Alkylation at the terminus of the

pentadienyl cation by ethylene would result in triene E. Although we did not observe triene E, acid-catalyzed isomerization of this intermediate would result in the observed 4-propyltoluene (6). If the intermediate B instead reacts with DMF in a Friedel–Crafts-type reaction, the observed major byproduct 12 arises. As in the reaction with ethylene, this electrophilic reaction would be expected to occur at the terminus of the extended cation, which is consistent with the observed products. Subsequent Diels–Alder reactions of 12 with ethylene, either at the dimethylfuryl group followed by dehydration or at the cyclohexadiene, lead to the formation of 20 and 18, respectively. We can exclude the direct formation of 20 from cation B because reactions performed with added *d*₁₀-*p*-xylene did not result in an increased deuterium content in 20, as judged by GC/MS (see the Supporting Information).

Finally, we have also observed several byproducts that are consistent with secondary oxidation of initially formed products. For example, the formation of 13 and 21 is readily explained by the aerobic oxidation of cyclohexadienes 12 and 20, respectively, after the reactor is opened to air.^{25,26} Likewise, dehydration of alcohol 14, followed by aerobic oxidation of the resulting diene, gives rise to substituted xylene 10.

3.3. Discussion of Reaction Network. The proposed reaction network is consistent with two major deleterious pathways leading to decreased yields of *p*-xylene. The first pathway involves the hydrolysis of DMF by water to generate 2,5-hexanedione (3). This side reaction is particularly plaguing because it not only consumes starting material, but the hydrolysis product is also subject to polymerization via aldol reactions in the acid environment. We believe that polymeric aldol byproducts from this pathway most likely explain the surface condensates observed at the end of the reaction and may also explain the darkening of the zeolite catalyst during the course of the reaction. Indeed, subsection of diketone 3 to the zeolite catalyst at 528 K resulted in considerable darkening of the catalyst surface, likely due to the formation of surface-bound polymers. Interestingly, however, very few soluble aldol-type products were observed in this control reaction, as determined by GC/MS analysis. This suggests that the hydrolysis pathway is not a significant contributor to the observed (soluble) product mixtures, as shown in Figure 2 and Table 1.²⁷

Unfortunately, because water is generated in the final step of the desired reaction pathway, complete suppression of the hydrolytic decomposition of DMF may be difficult to avoid. Further, it is clear from Table 1 that temperature plays a role in the hydrolytic reaction because more of diketone 3 is produced at higher temperatures, but this may simply be a result of greater conversion of DMF to *p*-xylene. One obvious strategy that may suppress the hydrolytic reaction is the removal or sequestration of water from the reaction media, such as by the addition of stoichiometric desiccants. Such studies will be undertaken in the near future.

The second nonproductive pathway involved in this reaction sequence appears to be a number of related Friedel–Crafts-type reactions resulting from side reactions of the highly electrophilic cationic intermediates en route to the product. Indeed, it appears that both allyl cation A as well as pentadienyl cation B participate in such side reactions. In particular, pentadienyl cation B appears to be a particularly serious branch point in the reaction network because it undergoes both Friedel–Crafts-type reactions (with ethylene or DMF). The increased stability of B, compared with A, due to its extended

conjugation would be expected to lead to a longer-lived intermediate. This stability and the resulting increase in steady state concentration may explain why more side products appear to derive from the latter intermediate.

In addition, one can easily envision a number of other regioisomeric byproducts arising from electrophilic reactions similar to those shown in Figure 3. The products from those pathways would be expected to provide compounds with similar or identical molecular formulas and mass spectroscopic fragmentation patterns highly similar to the identified compounds. As mentioned above, many of the unassigned compounds have GC/MS features closely resembling the Friedel–Crafts products shown in Figure 3; thus, we believe that the remaining byproducts also result from related electrophilic pathways.

Unfortunately, because the pathway leading to the desired *p*-xylene requires the intermediacy of both cations A and B, it is not possible to avoid the formation of these reactive intermediates. Likewise, one might consider controlling the concentration of the nucleophiles (i.e., ethylene and DMF) that participate in the electrophilic side reactions as a way to modulate the rates of formation of side products. However, both ethylene and DMF are required in the upstream Diels–Alder reaction, meaning that a reduction in their concentrations would likely have deleterious effects on the overall rate of *p*-xylene production. Consistent with this, we have previously observed that high operating pressures facilitate the rate of *p*-xylene production.⁴

Fortunately, however, the proposed reaction network does suggest a means for limiting the production of side products from electrophilic pathways. For both cations A and B, the undesired Friedel–Crafts-type pathways directly compete with productive deprotonation leading to *p*-xylene. One alternative is to use zeolite materials that contain higher concentrations of framework aluminum (i.e., lower Si/Al ratios), such as zeolite X, that are known to have lower effective acidity.²⁸ Alternatively, zeolites containing other framework heteroatoms (such as Ga(III) and Fe(III)) are also known to have lower effective acidity and could potentially aid in reducing the relative rates of the undesired reaction channels.^{29,30} Finally, an optimal selectivity window for *p*-xylene might be achieved by tuning the dielectric properties of the solvent. In fact, our previous results have shown that the use of *n*-heptane as solvent increases the selectivity of *p*-xylene from 55% to 75% on HY zeolite.⁴ One would expect that such a nonpolar solvent would destabilize cationic intermediates, which might result in a faster deprotonation step and increased rate of desired product formation. Future studies will be directed toward optimization of the zeolite catalyst as well as understanding solvent effects in the reaction.

4. CONCLUSION

Using advanced separation and analytical techniques, including extensive 1D and 2D NMR, we have been able to identify the majority of compounds produced in the reaction of 2,5-dimethylfuran (DMF) and ethylene over catalytic HY zeolite. In addition to the desired *p*-xylene, we have found that hydrolysis of the DMF and a number of electrophilic reactions of cationic intermediates lead to a range of side products. With detailed knowledge of byproduct structures, we have been able to propose a reaction network that is consistent with the observed product distribution. These studies suggest that active removal of water from the reaction, as well as the modulation of

the acidity of the zeolite catalyst, will result in higher selectivity for the desired *p*-xylene. This study constitutes one of the first examples of the application of modern analytical and separation techniques to understanding a reaction involved in the conversion of biomass-derived oxygenates into valuable feedstock products. We believe that application of such techniques to other problems in biomass conversion will have a significant and positive effect on developing more efficient and selective routes to commodity chemicals in the postpetroleum era.

■ ASSOCIATED CONTENT

● Supporting Information

Spectral data for isolated compounds. This material is available free of charge via the Internet at <http://pubs.acs.org>.

■ AUTHOR INFORMATION

Corresponding Author

*E-mail: dawatson@udel.edu (D.A.W.), lobo@udel.edu (R.F.L.).

Present Address

[§]UOP-Honeywell Research Center, 50 E. Algonquin Rd., Des Plaines, IL 60017.

Author Contributions

[†]These authors contributed equally.

Notes

The authors declare no competing financial interest.

■ ACKNOWLEDGMENTS

Data were acquired on instruments obtained via NSF and NIH funding (NSF MIR 0421224 and CRIF MU CHE0840401, NIH P20 RR017716). This work was supported as part of the Catalysis Center for Energy Innovation, an Energy Frontier Research Center funded by the US Department of Energy, Office of Basic Energy Sciences under Award No. DE-SC0001004

■ REFERENCES

- (1) *BP Statistical Review of World Energy*; British Petroleum: London, 2012.
- (2) Sanderson, K. *Nature* **2006**, *444*, 673.
- (3) Mettler, M. S.; Vlachos, D. G.; Dauenhauer, P. J. *Energy Environ. Sci.* **2012**, *5*, 7797.
- (4) Williams, C. L.; Chang, C.-C.; Do, P.; Nikbin, N.; Caratzoulas, S.; Vlachos, D. G.; Lobo, R. F.; Fan, W.; Dauenhauer, P. J. *ACS Catal.* **2012**, *2*, 935.
- (5) Lin, Y.-C.; Huber, G. W. *Energy Environ. Sci.* **2009**, *2*, 68.
- (6) FitzPatrick, M.; Champagne, P.; Cunningham, M. F.; Whitney, R. A. *Bioresour. Technol.* **2010**, *101*, 8915.
- (7) Binder, J. B.; Raines, R. T. *J. Am. Chem. Soc.* **2009**, *131*, 1979.
- (8) Fabri, J.; Graeser, U.; Simo, T. A. In *Ullmann's Encyclopedia of Industrial Chemistry*; Wiley-VCH Verlag GmbH & Co. KGaA: Weinheim, 2000.
- (9) Brandvold, T. A. Honeywell/UOP; US Patent Application 2010/0331568 A1, 2010.
- (10) Shiramizu, M.; Toste, F. D. *Chem.—Eur. J.* **2011**, *17*, 12452.
- (11) Zhang, Z. C.; Brown, H. M.; Su, Y. Battelle Memorial Institute, Columbus, OH; US Patent 8,110,667 B2, 2009.
- (12) Patwardhan, P. R.; Satrio, J. A.; Brown, R. C.; Shanks, B. H. *J. Anal. Appl. Pyrol.* **2009**, *86*, 323.
- (13) Chidambaram, M.; Bell, A. T. *Green Chem.* **2010**, *12*, 1253.
- (14) *Basic Research Needs: Catalysis for Energy*; The U.S. Department of Energy, Office of Basic Energy Sciences Workshop, Bethesda, MD; Aug 6–8, 2007.

(15) Kalsi, P. S. *Spectroscopy of Organic Compounds*; New Age International (P) Ltd.: Tunbridge Wells, U.K., 2007.

(16) Claridge, T. D. W. *High-Resolution NMR Techniques in Organic Chemistry*; Elsevier Science: London, Amsterdam, 2008.

(17) *NMR Spectroscopy in Pharmaceutical Analysis*; Wawer, I.; Diehl, B.; Holzgrabe, U., Eds.; Elsevier Science: Oxford, 2008.

(18) *Bioactive Natural Products: Detection, Isolation, and Structural Determination*, 2nd ed.; Colegate, S. M.; Molyneux, R. J., Eds.; Taylor & Francis: 2007.

(19) Hübschmann, H. J. *Handbook of GC/MS: Fundamentals and Applications*; John Wiley & Sons: New York, 2008.

(20) González Maldonado, G. M.; Assary, R. S.; Dumesic, J.; Curtiss, L. A. *Energy Environ. Sci.* **2012**, *5*, 6981.

(21) Ronsse, F.; Bai, X.; Prins, W.; Brown, R. C. *Environ. Prog. Sustainable Energy* **2012**, *31*, 256.

(22) Reactions run to higher levels of conversion contained similar, although somewhat more complex, mixtures of byproducts (as judged by GC/MS). We believe that the increase in complexity of the byproducts under these conditions is predominately due to further reactions of the side products facilitated by longer reaction times.

(23) Dessau, R. M. *J. Chem. Soc., Chem. Commun.* **1986**, *15*, 1167.

(24) Stamhuis, E. J.; Drenth, W.; Van den Berg, H. *Recl. Trav. Chim. Pays-Bas* **1964**, *83*, 167.

(25) Hendry, D. G.; Schuetzle, D. *J. Am. Chem. Soc.* **1975**, *97*, 7123.

(26) McGraw, G. W.; Hemingway, R. W.; Ingram, L. L.; Canady, C. S.; McGraw, W. B. *Environ. Sci. Technol.* **1999**, *33*, 4029.

(27) Other byproducts resulting from the self-reaction of either DMF or ethylene were not detected.

(28) Ravenelle, R. M.; Schüssler, F.; D'Amico, A.; Danilina, N.; van Bokhoven, J. A.; Lercher, J. A.; Jones, C. W.; Sievers, C. *J. Phys. Chem. C* **2010**, *114*, 19582–19595.

(29) Corma, A. *Chem. Rev.* **1995**, *95*, 559.

(30) Shamzhy, M. V.; Shvets, O. V.; Opanasenko, M. V.; Yaremov, P. S.; Sarkisyan, L. G.; Chlubná, P.; Zúkal, A.; Marthala, V. R.; Hartmann, M.; Čejka, J. *J. Mater. Chem.* **2012**, *22*, 15793.